

Transmission Electron Microscopy Imaging of Structural Transformation Dynamics in a Single Nanocrystal

Haimei Zheng

Materials Sciences Division, Lawrence Berkeley National Laboratory, 1 Cyclotron Road, Berkeley, CA 94720

hmzheng@lbl.gov

Introduction

Over the last decade, transmission electron microscopy (TEM) has advanced remarkably. With the development of aberration-corrected optics, improved recording systems, high brightness guns, and so on, imaging with single-atom sensitivity across the periodic table has become a reality. Atomic resolution imaging with rapid acquisition and with greater signal collection efficiency opens many opportunities in the study of dynamic processes of materials.

Recently, using one of the world's most powerful aberration-corrected TEMs (TEAM0.5, see Figure 1), the transient structural transformation dynamics of a single nanocrystal has been imaged *in situ* with atomic resolution [1]. That work revealed an unprecedented level of detail on the fluctuation dynamics during phase transition, including phase nucleation, phase propagation, pinning of structural domains by defects, and so on. These observations provide critical insights into the atomic pathway of phase transitions, which can aid in the design of materials with improved properties. This article reviews the main findings from the work on the phase transition of a single Cu_2S nanorod and provides a perspective on future real-time imaging of materials transformations using a TEM.

First-Order Phase Transitions in Small Systems

First-order phase transitions in solids play an important role in a variety of processes. First-order phase transitions are characterized by discontinuities in the first derivatives of the free energy. Many structural transformations in solids fall into this category, where the system absorbs or releases a fixed amount of energy (latent heat or specific heat) without changing temperature at the transition. For example, bulk copper sulfide crystal (Cu_2S) transforms from the monoclinic low-chalcocite phase to the hexagonal high-chalcocite phase at 376 K with a specific heat of $\Delta\varepsilon = 3849$ J/mole.

In nanoscale systems, characteristics of phase transitions can be distinctly different from the bulk [2, 3]. The temperature at which the phase transition occurs broadens in small systems in contrast to the sharp transition point of bulk materials. The distinctive feature of the first-order phase transition is phase coexistence at the transition. According to the phase transition theory, the energetic barrier to a structural transformation scales with crystal size. When the size of a nanocrystal is in a regime where thermal energy is comparable to the energy barrier for the phase transformation, fluctuations between two the stable structures occur at the transition. Therefore, the specific heat is no longer a fixed value (the configuration is dependent on the crystal size). In addition, the discontinuities at a first-order transition are smeared out, and there is no unambiguous way by which one can detect the order.

There has been significant interest in understanding first-order phase transitions in small systems, especially the fluctuation characteristics of structural transformations in nanocrystals. Also, there have been numerous previous studies on phase transitions in nanocrystals [4, 5]. However, in most ensemble experiments, only the average characteristics of the fluctuations can be observed, and many important features may be completely obscured by parallel, unsynchronized transition processes. Direct imaging of the dynamic structural transformations in a single nanocrystal provides the opportunity to reveal the nature of the first-order phase transition. Structural transformations between low- and high-chalcocite phases in a single Cu_2S



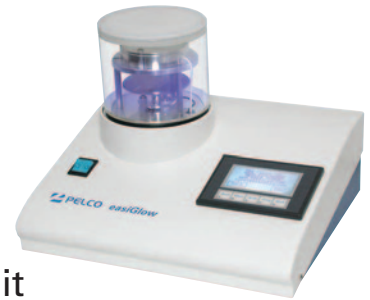
Figure 1: The aberration-corrected microscope (TEAM0.5) was used for this work.

Preparation Equipment and Microscopy Supplies

The single source for All your microscopy supplies and specimen preparation equipment.



- Vacuum Coating Systems
- Calibration Standards
- PELCO® easiGlow™ Glow Discharge Unit
- SEM Sample Holders and Mounts
- Silicon Nitride TEM Membranes
- PELCO BioWave Pro® Tissue Processor
- TEM Support Films



- AFM Supplies
- Quality Laboratory Tweezers
- Vacuum Pick-up Systems
- Digital Stereo Microscopes
- Conductive Adhesives
- FIB Supplies



Complete line of compact Cressington EM Sample Coaters.

TED PELLA, INC.
Microscopy Products for Science and Industry

sales@tedpella.com

800-237-3526

www.tedpella.com

nanocrystal have been studied *in situ* using the state-of-art TEAM0.5 microscope.

Materials and Methods

Samples for TEM investigation were prepared by drop-casting a dilute solution of Cu₂S nanorods on a conductive carbon grid (purchased from Ted Pella, Inc.). The Cu₂S nanorods were synthesized through a colloidal solution process and have diameters of 5 nm and lengths of 20–40 nm. The Cu₂S nanorods exhibit the low-chalcocite phase at room temperature. At 337 ± 4 K, Cu₂S nanorods transform to the high-chalcocite structure, during which the hexagonal sulfur sublattice remains rigid but copper atoms occupy different lattice sites. The measured transition temperature of Cu₂S nanorods (5 nm in diameter) is lower than that of the bulk crystal determined by variable-temperature X-ray diffraction studies.

While imaging in the TEM, part of the energy dissipated from the interaction between the nanocrystal and the electron-beam (for example, inelastic scattering of the incident electrons) was converted into heat. Because the phase transition temperature of the Cu₂S nanorods is relatively low (337 ± 4 K), heating from the electron beam can be used to induce structural transformations. A series of high-resolution TEM images of a Cu₂S nanorod were recorded continuously at a rate of 0.5 s per frame using the TEAM0.5 microscope operated at 80 kV. During recording, a current density of $\sim 5000 \text{ e}\cdot\text{\AA}^{-2}\cdot\text{s}^{-1}$ was maintained. The microscope was tuned to a condition such that the atomic structures of the two phases could be resolved in a single image. For example, a spherical aberration (Cs) value of -0.015 mm was used and the defocus was set to around 8 nm. Under these conditions, atomic columns appear bright, and the intensities reflect different atoms within a crystal lattice as long as the surface roughness of the sample does not significantly exceed the focal spread in the beam direction ($\sim 1 \text{ nm}$) [6].

Results

Figures 2A I and 2B I are TEM images of a Cu₂S nanorod recorded with the above conditions. They are the enlarged sections from a single nanorod showing both high- and low-chalcocite phases. The nanorod was at an intermediate transition state with a low-chalcocite core forming inside the high-chalcocite shell. Figure 2A I–IV show that the atomic structure of high-chalcocite phase from the experiment matches well with the simulated phase image and the structural model. Because of the core-shell geometry, the projection of the overlapping low- and high-chalcocite phases is observed in Figure 2B I. However, a well-defined low-chalcocite structure can still be identified.

For comparison, several through focus image series were recorded for exit wave reconstruction [7], and these led to atomic phase images of a Cu₂S nanorod before and after the phase transition. The MacTempas image simulation program (<http://www.totalresolution.com>) was used for image simulation. Phase images after exit wave reconstruction (Figure 2 II) show sharper contrast compared with the single images (Figure 2 I). However, because the atomic structural information is well retained in the single image and the phase transition is dynamic in nature, the image series collected at

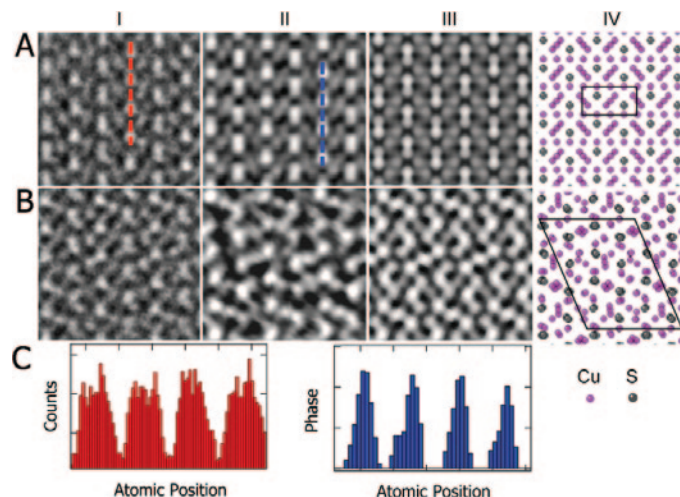


Figure 2: Single high-resolution TEM images of low- and high-chalcocite structures (I) and phase images by exit wave reconstruction of through-focus image series (II). (A) High-chalcocite phase. (B) Low-chalcocite phase. In both (A) and (B), (I) is the experimental image, (II) is the phase image by exit wave reconstruction, (III) is the simulated phase image, (IV) is the structural model. (C) Atomic profiles corresponding to the vertical red and blue lines in (A).

constant focus (with the above optimum imaging conditions) was used for the study of Cu₂S phase transition.

An image-processing technique was developed to visualize the structural changes of a Cu₂S nanorod. As shown in Figure 3, digital masks that are characteristic of the two phases were applied in Fourier space. The corresponding filtered real-space images allow identification of the low-chalcocite or high-chalcocite domains in a single nanocrystal. For noise reduction, our mask design captures only Fourier components above a given threshold (for example, signal/noise > 10). As a consequence, some information is lost during image process. Therefore, the filtered images do not represent the measured copper distribution in the two phases but, rather, reflect the size and shape of the structural domains. The MacTempas image simulation program was used for image processing, and Adobe Photoshop software was used for false coloring of the images. By applying the image process to the time series of high-resolution TEM images, dynamic structural transformations within a single Cu₂S nanorod can be tracked in time.

Fluctuations and Transient Structures

Trajectories of the structural transformation in a single-crystal Cu₂S nanorod show that Cu₂S transformed from an initial low-chalcocite structure to a transition state where either the complete Cu₂S nanorod or a portion of it temporarily transformed into high-chalcocite, and the two structures were fluctuating back and forth, eventually forming a stable high-chalcocite. The duration during which fluctuations were observed in a nanorod increased (or decreased) with the decrease (or increase) of the electron current density. Under the above imaging conditions, the average duration of fluctuations was a few seconds for single-crystal Cu₂S nanorods.

The structural transformation dynamics of Cu₂S nanorods was strongly affected by the presence of defects. For example, a stacking fault across a Cu₂S nanorod separated the nanorod into different structural domains (Figure 4). Trajectories of

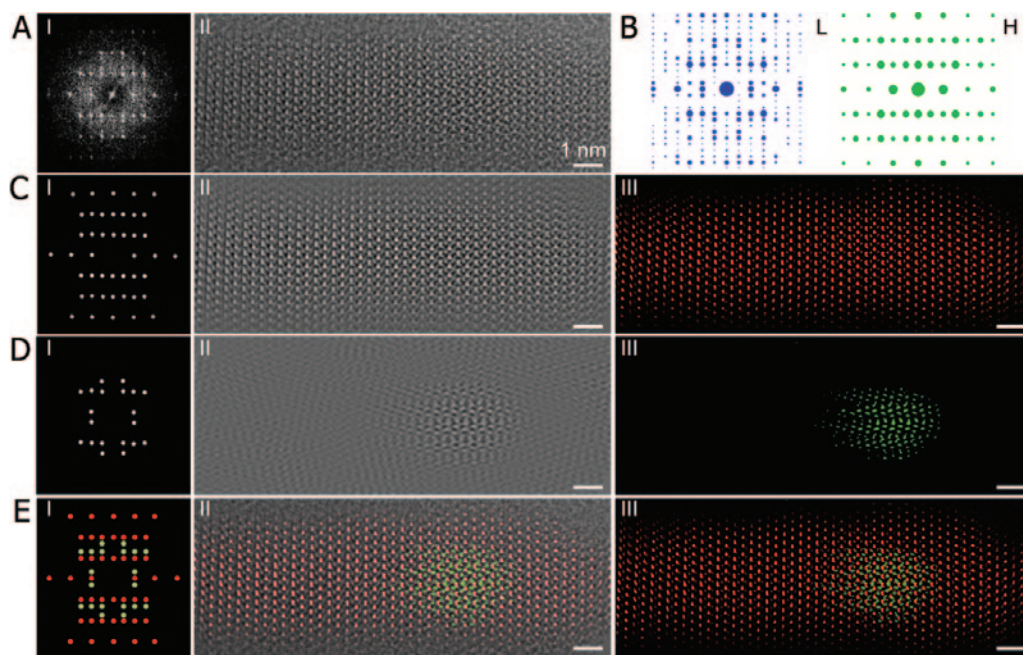


Figure 3: Images and image processing to visualize the low- and high-chalcocite structures in a Cu_2S nanorod. (A) High-resolution TEM image of the Cu_2S nanorod (II) and the corresponding FFT pattern (I). (B) Diffraction patterns of low-chalcocite along the [010] zone axis (L) and of high-chalcocite along the [110] zone axis (H). (C) Mask placed in the FFT pattern of (A) allowing the diffraction spots from the hexagonal lattice to pass (I). The corresponding filtered image shows the high-chalcocite domain or the hexagonal lattice frame of low-chalcocite (III) corresponding to (II). (D) Mask placed in the FFT pattern of (A) allowing the low-chalcocite diffraction spots to pass (I). The corresponding filtered image (II) shows the low-chalcocite domain. False color image (III) corresponding to (II). (E) (I) The overlapping of the two masks in (C) and (D). (II) The overlapping of the color image of (III) and the original image in (A). (III) The two structures in the nanorod highlighted by overlapping the two color images in (C) and (D).

structural fluctuations are different in adjacent domains. A higher fluctuation frequency was observed in the smaller domain (Zone II) in Figure 4B. It is likely that there were rapid structural fluctuations of even smaller domains during the nucleation process.

Characteristics of phase nucleation and phase propagation were different for the forward and reverse transformations. At the onset of the transition from low-chalcocite to high-chalcocite, the high-chalcocite structure was at the outer surface of the low-chalcocite nanorod (Figure 4A). The high-chalcocite propagated inward until the whole nanorod was transformed into pure high-chalcocite. When the low-chalcocite phase reappeared (nucleated), it was located at the core of the high-chalcocite Cu_2S nanorod. The low-chalcocite domain propagated along the long-axis of the nanorod or grew into a larger domain, which suggests the transition from high-chalcocite to low-chalcocite is a nucleation and growth process.

The fluctuation kinetics has been estimated using a thermodynamic fluctuation model. The duration of the fluctuations τ can be expressed as:

$$\tau = \tau_0 e^{E_s/2k_B T^2 C} \quad (1)$$

where τ_0 is an attempt time for the atoms to execute the transition, which is usually taken as a vibrational period and is on the order of picoseconds. E_s is the interfacial energy between high- and low-chalcocite phases, which results from the different Cu arrangements in these two phases

and the related extra Ewald energy at the interface. The interfacial energy between low- and high-chalcocite is approximately the same as the internal energy difference between these two phases [8], $(\epsilon_1 - \epsilon_2) = 40$ meV per unit cell [9]. Assuming the low-chalcocite Cu_2S of N formulae units form a spherical core within a large reservoir of high-chalcocite, we have: $E_s = (36\pi)^{1/3} N^{2/3} (\epsilon_1 - \epsilon_2)$. Note that $C = C_{\text{unit}} N$, and $C_{\text{unit}} = 52$ J/mole·K [9]. Thus, from Eq. (1), we get $\tau \sim 2$ seconds when $N = 1000$ (2–4 nm domain size) and $\tau_0 = 1$ ps [10]. This fluctuation time is of the same order as our observed experimental value.

Discussion

It is expected that the features from this observation will be of interest to the community that attempts to simulate structural transformations in solids, because details of the fluctuations

between two phases have never before been available. This also implies that strategies such as blocking or creating free surfaces in the nanomaterials may be considered as a means of suppressing or assisting the phase transformation. In addition, because Cu_2S phase transition is associated with the transport of copper ions within a sulfur crystal lattice frame, our observation is highly relevant to questions on how ion transport occurs within electrodes during charge and discharge of batteries.

In situ TEM studies of materials transformations play an increasingly important role in basic sciences and energy research frontiers. Despite the significant advances in TEM resolution, real-time imaging of structural dynamics opens new chapters for technical development. For example, because many materials reactions are in a liquid or gas environment or under electric biasing, sample stability, sensitivity regarding signal-to-noise ratio, and the repeatability of the observations are topics for future development. In addition, although the electron beam is essential for TEM imaging, its perturbation to materials processes resulting from the energy deposition is an important issue. Low-dose imaging techniques (such as those for imaging biological samples) or imaging with low voltages (to minimize the knock on damage) may eliminate or control the electron beam effects. There is no doubt TEM will remain a powerful tool and continue to advance for years to come.

Conclusions

In summary, dynamic structural transformations of a single Cu_2S nanorod from a low-chalcocite to a high-chalcocite

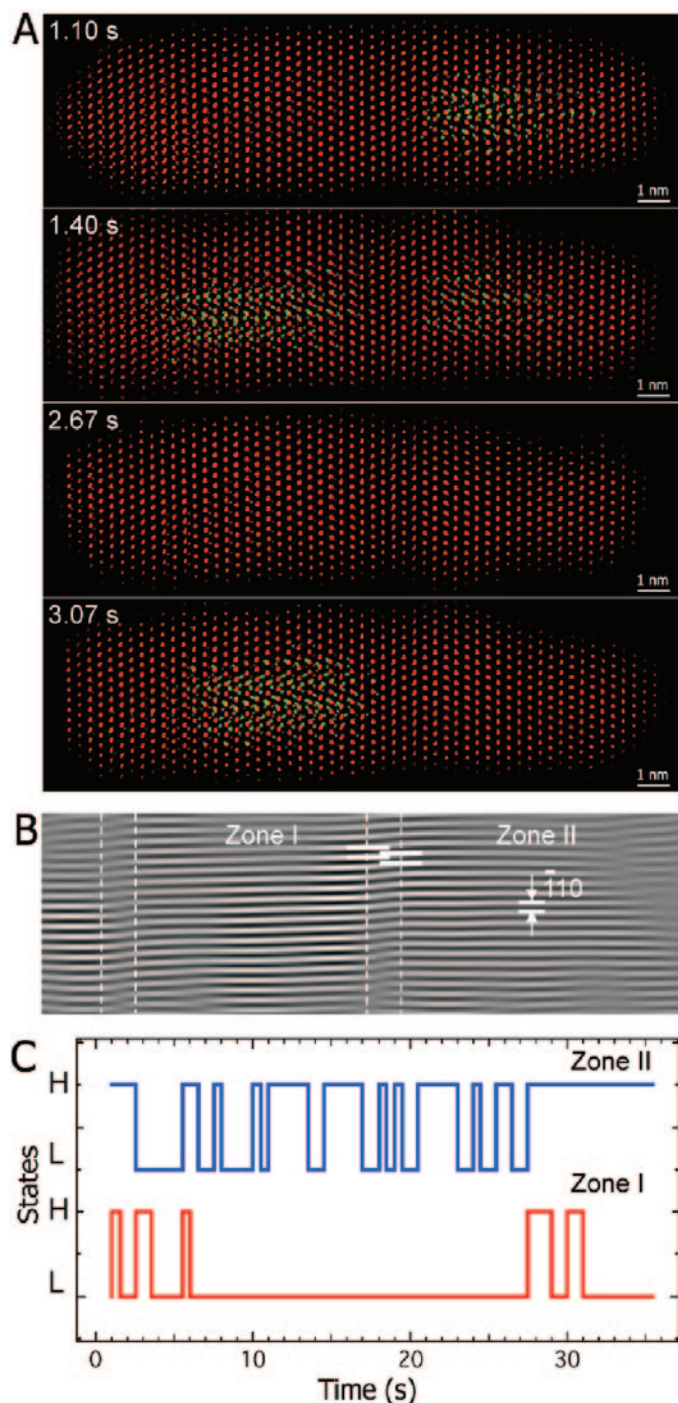


Figure 4: Trajectories of structural transformation in a Cu_2S nanorod and the effect of defects. (A) Sequential images showing the low-chalcocite structure (green; L), mixed structure (mixed green and red domains; L), and the pure high-chalcocite structure (red; H). (B) Filtered image showing $(\bar{1}10)$ planes, where the regions marked with dashed lines highlight a stacking fault. (C) Trajectories of structural fluctuations in Zone I and Zone II during the transition period.

structure have been observed *in situ* by TEM: (a) the high-chalcocite phase initiates on the outer surface of a Cu_2S nanorod while low-chalcocite nucleates within the core during the transition, (b) the propagation of phases results from copper ions moving within a sulfur sublattice, and (c) defects have strong effects on the transition. This work provides critical insights into the microscopic pathways of the phase

transition. Because complex phase transition kinetics occurs in bulk materials or nanocrystal ensembles because of the parallel phase transition processes in different parts of the sample, the single nanorod study presents an ideal case where fluctuations in one or only a few domains along the length of the nanorod can be monitored.

References

- [1] HM Zheng, JB Rivest, TA Miller, B Sadtler, A Lindenberg, MF Toney, LW Wang, C Kisielowski, and AP Alivisatos, *Science* 333 (2011) 206–09.
- [2] LD Landau, EM Lifshitz, *Statistical Physics*, Pergamon Press, New York, 1980.
- [3] MSS Challa, DP Landau, K Binder, *Phys Rev B* 34 (1986) 1841–52.
- [4] K Jacobs, D Zaziski, EC Scher, AB Herhold, AP Alivisatos, *Science* 293 (2001) 1803–06.
- [5] ZW Wang, XD Wen, R Hoffmann, JS Son, RP Li, CC Fang, DM Smilgies, T Hyeon, *P Natl Acad Sci USA* 107 (2010) 17119–24.
- [6] R Erni, MD Rossell, MT Nguyen, S Blankenburg, D Passerone, *Phys Rev B* 82 (2010) 165443.
- [7] W Coene, G Janssen, MO Debeek, D Vandyck, *Phys Rev Lett* 69 (1992) 3743–46.
- [8] F Glas, *J Appl Phys* 104 (2008) 093520.
- [9] DJ Chakrabarti and DE Laughlin, *Bulletin of Alloy Phase Diagrams* 4 (1983) 254.
- [10] AF Voter, *Phys Rev B* 34 (1986) 6819–29.

MT

The Next Generation Critical Point Dryer

New! **931.GL SAMDRI®**

tousimis

Tel. 301.881.2450 / Web. www.tousimis.com / Email. trc@tousimis.com

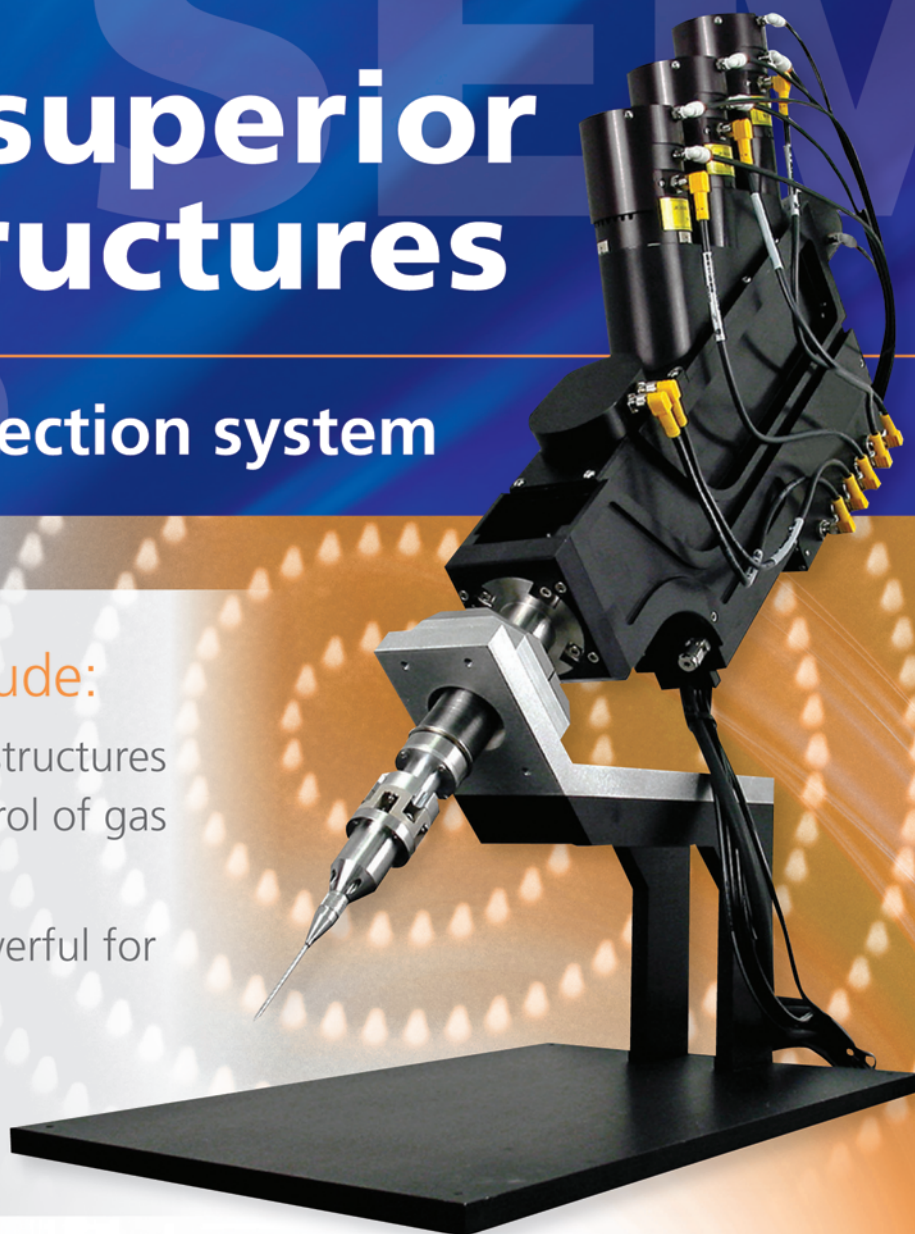
Building with Resources CPD Processed by Fully Automated, Automated P. 810, Series A / Dwayne E. K. University of Missouri, EM Core Facility

Create superior nanostructures

Multiple gas injection system

Unique benefits include:

- Higher resolution nanostructures through advanced control of gas flow and mixture
- Easy for beginners, powerful for advanced research
- Free up ports on your SEM/FIB



OmniGIS®

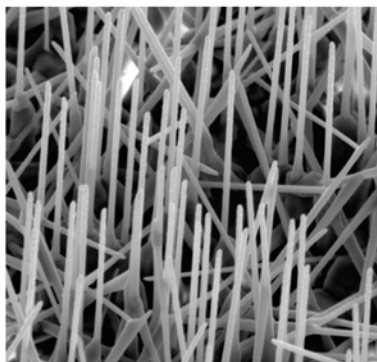
Scan the QR code below to discover more

mtme.me/519da6



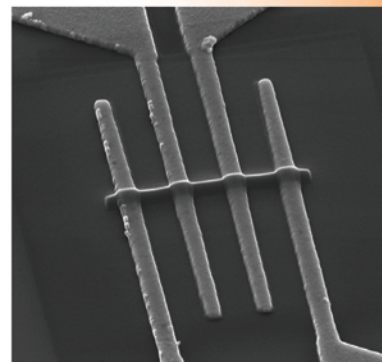
Email: omniprobe@oxinst.com
www.oxinst.com/omniprobe

Modify



ALD surface alteration

Make



Better electrical connections

 **omniprobe®**
An Oxford Instruments Company

OXFORD
INSTRUMENTS
The Business of Science®